

Measurement of Z Boson Transverse Momentum at the Fermilab Tevatron Collider

The DØ Collaboration
(Dated: July 26, 2006)

We present preliminary results on the inclusive differential cross section as a function of boson transverse momentum in an invariant mass range between 70 and 110 GeV/c^2 . The data was collected by the DØ detector at Fermilab's Tevatron $p\bar{p}$ collider, operating at $\sqrt{s}=1.96$ TeV, and corresponds to a total integrated luminosity of 960 pb^{-1} .

I. INTRODUCTION

At the Tevatron, at leading order, the weak bosons (W and Z) are mostly produced via the annihilation of quarks and anti-quarks. At NLO in α_s , the weak bosons have transverse momentum relative to the beam axis because of gluon bremsstrahlung off the initial quarks and boson production via the gluon compton scattering diagram. The differential cross section of the weak boson can not be calculated at finite order in perturbative QCD at very low transverse momentum, where multiple soft gluon radiation dominates and the calculation diverges. A technique for including higher order diagrams in the calculation, called resummation, was developed by Collins, Soper and Sterman (CSS)[1], which gives a finite result. C. Balazs and C.P. Yuan[2] developed the CSS formalism by calculating the effects of multiple soft gluon radiation on the distributions of the decay leptons. However, this model does have some sensitivity to non-perturbative physics via an ansatz-function containing three parameters which must be determined from experimental data. One of the most sensitive observables to these effects is the Z boson transverse momentum. A precision measurement of the Z boson transverse momentum will not only provide a sensitive test of the theory for weak boson production, it will also help reduce the theoretical uncertainty on the precision W mass measurement. Previous measurements from the Run I data have been published by DØ [3] and CDF [4] using around 100 pb^{-1} data. With about 1 fb^{-1} data collected by DØ during Run II, a much more precise measurement can now be done.

Stefan Berge et al.[5], based on an updated resummation technique developed to understand the p_T distributions in semi-inclusive deep inelastic scattering data, predicts a small- x broadening of the Z p_T distribution might occur in forward Z boson production, compared to the standard CSS calculation. With about 1 fb^{-1} data, and more than 5000 forward Z bosons, a preliminary test of this prediction can be done.

II. THE DØ DETECTOR AND THE DATA SAMPLE

The DØ detector is described elsewhere[6]. It includes a central tracking system, composed of a silicon microstrip tracking (SMT) and a central fiber tracker (CFT), both located within a 2 T superconducting solenoidal magnet and optimized for tracking and vertexing capability at pseudorapidities of $|\eta| < 2.5$. Three liquid argon and uranium calorimeters provide coverage out to $|\eta| \approx 4.2$: a central section covering $|\eta|$ up to ≈ 1.1 , and two endcap calorimeters. A muon system resides beyond the calorimetry, and consists of tracking detectors, scintillation counters, and a 1.8 T toroid with coverage for $|\eta| < 2$. Luminosity is measured using scintillator arrays located in front of the endcap calorimeter cryostats, covering $2.7 < |\eta| < 4.4$. Trigger and data acquisition systems are designed to accommodate the high luminosities of the Run II Tevatron.

The data sample used in this analysis was taken between Oct 2002 and Nov 2005. The integrated luminosity for this sample is approximately 960 pb^{-1} .

III. EVENT SELECTION

Our selection criteria for candidate Z bosons requires two isolated electromagnetic (EM) clusters in the calorimeters that pass electron identification criteria, have high transverse momenta, and an invariant mass consistent with that of the Z boson.

Electromagnetic (EM) candidates are required to have a high electromagnetic fraction, defined as

$$f_{EM} = \frac{E_{EM}}{E_{EM} + E_{Had}} \quad (1)$$

where E_{EM} and E_{Had} are EM energy and hadronic energy measured by the EM and hadronic calorimeters, respectively.

The isolation variable is defined as:

$$f_{iso} = \frac{E_{tot}(0.4) - E_{EM}(0.2)}{E_{EM}(0.2)} \quad (2)$$

where $E_{tot}(\mathcal{R})$ and $E_{EM}(\mathcal{R})$ are total energy and EM energy, respectively, in the cone with radius $\mathcal{R} = \sqrt{(\Delta\eta)^2 + (\Delta\phi)^2}$, around the candidate electron.

To select $Z/\gamma^* \rightarrow e^+e^-$ events, we require two high p_T electron candidates, each satisfying the following single EM requirements:

- $|\eta_{det}| < 1.1$ [7] (Central Calorimeter) or $1.5 < |\eta_{det}| < 3.2$ (End Cap Calorimeter)

- Transverse energy (E_T) >25 GeV
- $f_{EM} >0.9$, $f_{iso} <0.15$
- not near boundaries of the calorimeter modules or in regions of the calorimeter with malfunctioning electronics
- shower shape consistent with that expected for an electromagnetic shower (H-matrix selection)

Events with both candidate electrons in the central calorimeter are referred to as CCCC events; those with one in the central calorimeter and one in an endcap calorimeter as CCEC events; those with both candidate electrons in the endcap calorimeter as ECEC events.

In addition, our Z boson candidate selection requires:

- for CCCC events, both electron candidates have a track in the tracking system that extrapolates to the position of the cluster in the calorimeter (within the uncertainties in the two positions);
- for CCEC and ECEC events, at least one electron has a matching track;
- the invariant mass of the two electrons is between $[70,110]$ GeV;
- at least one of the two electrons fired one of the online electron triggers (These triggers typically require an isolated electromagnetic cluster with transverse energy greater than a threshold that varied with time and run conditions, but was always less than 22 GeV.).

After these requirements, 63901 events are selected as Z/γ^* candidates. Table I shows the selection results.

CCCC	CCEC	ECEC	All
23959	30344	9598	63901

TABLE I: Number of events that pass the selection requirements with both candidate electrons in the central calorimeter (CCCC), one in the central and one in the endcap (CCEC), and with both candidate electrons in the endcap calorimeter (ECEC).

IV. ELECTRON SELECTION EFFICIENCIES

Efficiencies are measured from the data using the tag and probe method. The tag electron is always required to pass all the single EM requirements and the trigger requirement. For all tag and probe efficiencies, if both electrons pass the tag selection requirements then they are both considered as tags as well as probes. Efficiencies are applied in the following order:

- isolation and f_{EM} efficiency
- Spatial track matching efficiency
- Trigger efficiency
- H-matrix efficiency

Efficiencies are parameterized in terms of the electron E_T and detector pseudorapidity (η_{det}).

Probe electrons must pass all the requirements of all previous selections. The effect of background needs to be taken into account when the isolation and spatial track-matching efficiencies are measured. But for the trigger and H-matrix efficiencies, since these are relative to the spatial track match efficiency, the level of background is very small.

The average isolation efficiency for electron candidates in the central calorimeter is $99.6\pm 0.1\%$; it is $99.2\pm 0.1\%$ for electron candidates in the endcap calorimeters. The isolation efficiency also depends on the transverse momentum of the Z boson. This dependency is studied using a full GEANT [8]-based simulation of the DØ detector, and has its minimum value at a Z p_T of around 40 GeV/c.

The spatial track matching efficiency depends on the z position of the primary vertex, in addition to the electron E_T and η_{det} . The tracking efficiency depends on the exit radius of the track from the tracking system, which is larger, for a fixed electron η , when the z vertex position is farther from the calorimeter.

The trigger efficiency is on average between 96.6% to 99.0%, depending on the trigger condition at the time.

The average H-matrix efficiency is 97.1% for electron candidates in the central calorimeter and 96.9% for candidates in the endcap calorimeter.

V. MONTE CARLO SIMULATION

We use ResBos[9] and PHOTOS[10] as the Z/γ^* event generator. ResBos is a Monte Carlo for Resummed Boson Production and Decay. It is used to compute the differential cross section $\frac{d^2\sigma}{dp_T dy}$ for processes $p\bar{p} \rightarrow B(\rightarrow l_1 l_2)$ with soft-gluon resummed initial state QCD corrections included. Here B is a boson (W^\pm, Z, γ^* ...) and l_1, l_2 are leptons. PHOTOS is a Monte Carlo program for QED single-photon radiative corrections in decays. Here it is used to apply final state QED radiation to Z/γ^* decays.

We use a parameterized Monte Carlo simulation (PMCS) to simulate the effect of the detector smearing and to include the measured electron identification efficiencies. We also include the merging of energies deposited by QED photons and electrons in the simulation. The electron energy scale and resolutions are tuned using the Z data, after correction for background contamination.

Figures 1, 2 show the data/Monte Carlo comparison for the Z/γ^* invariant mass and rapidity distributions. These plots also include the contribution from the background (described in Section VI). For these plots, the Resbos parameters were set to their default values. These parameters will be retuned using the results from this measurement in the near future.

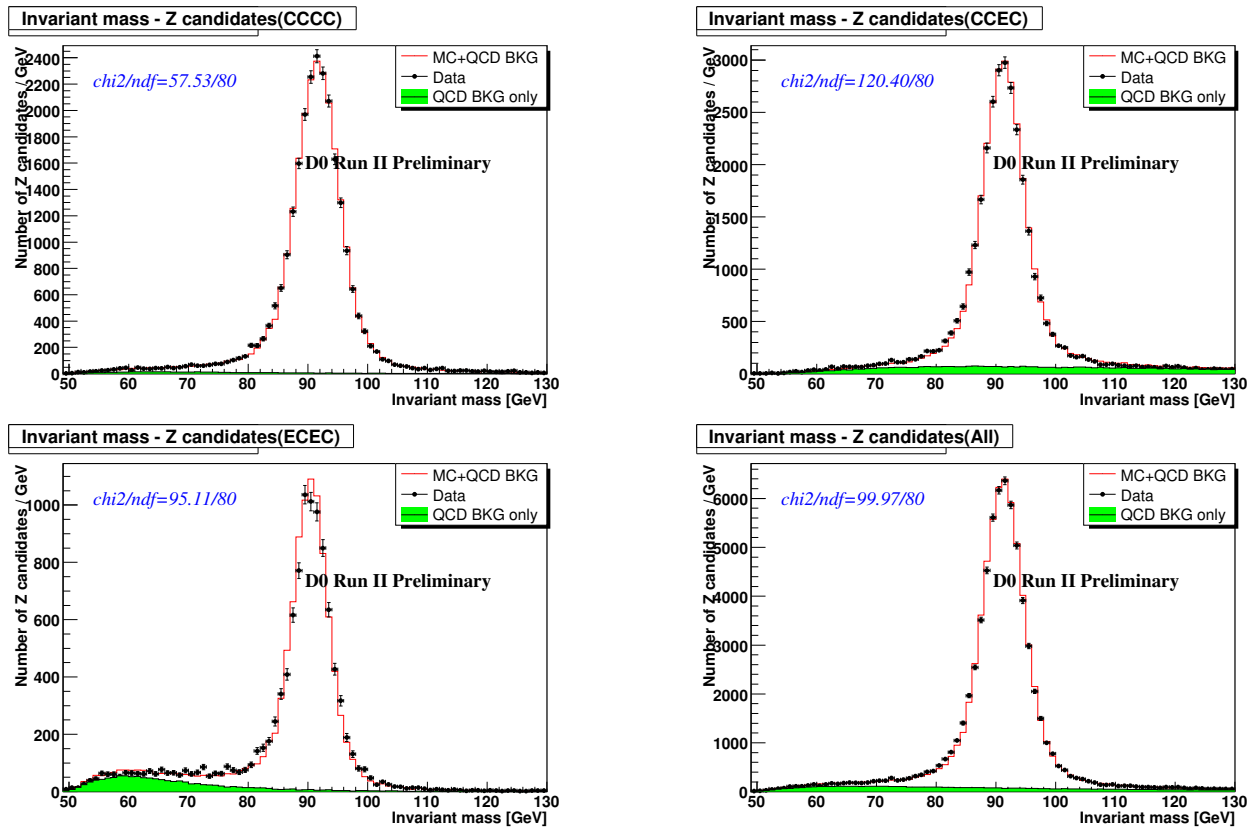


FIG. 1: Invariant mass distribution for data and Monte Carlo of $Z/\gamma^* \rightarrow e^+e^-$ events. The green areas correspond to backgrounds.

VI. BACKGROUND

The following processes can contribute background to the Z/γ^* sample:

- QCD background where one or two jets fake electrons;
- $Z \rightarrow \tau^+\tau^- \rightarrow e^+e^- \nu_\tau \nu_e \bar{\nu}_\tau \bar{\nu}_e$;
- WZ events, when the Z decays $Z \rightarrow e^+e^-$;

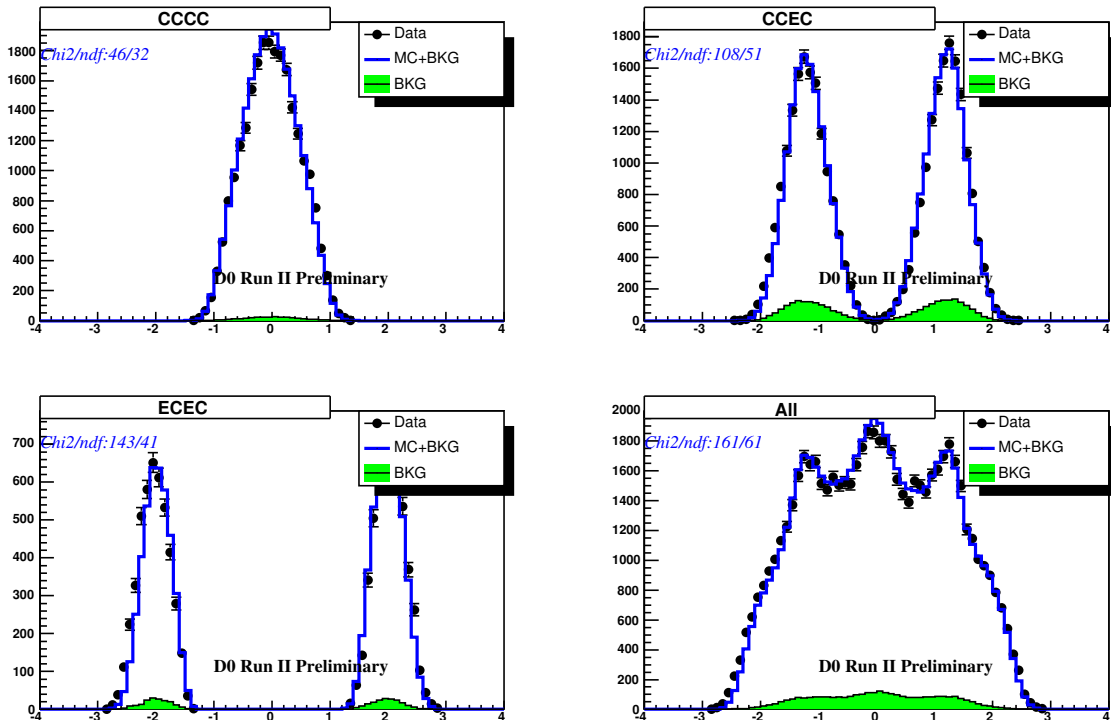


FIG. 2: Rapidity distribution for CCCC, CCEC, ECEC, All data and Monte Carlo Z/γ^* events. The green areas correspond to backgrounds.

- $W^+W^- \rightarrow e^+e^-\nu_e\bar{\nu}_e$ events;
- $W\gamma$ when the W decays $W \rightarrow e\nu$ and the photon is mis-identified as an electron.

The QCD backgrounds include di-jet events and EM+jet (direct γ , W +jet) events. To estimate the size of this background, samples that contain mostly background events, such as electromagnetic clusters that fail the electron selection criteria, or electromagnetic cluster plus jet events, are used to get the shape of the invariant mass distribution from this source. The shapes of the mass distributions from these samples are found not to depend very much on what selections are used, and are shown as the green curves in Figure 1. The invariant mass distribution from the data sample is then fit as a linear combination of this shape and the shape from the simulation of the signal. Table II shows the background fraction for events in the different calorimeter regions.

Region	background fraction
CCCC	1.30%
CCEC	8.69%
ECEC	3.79%
All	4.98%

TABLE II: Background fractions for events in different calorimeter regions.

For the other sources of background: $Z \rightarrow \tau^+\tau^-$ and diboson ($WW, WZ, W\gamma$) production, their contributions were studied using Monte Carlo simulation, and are found to be negligible.

VII. UNFOLDING

The measured Z boson p_T spectrum is smeared due to detector resolution effects. To be able to compare with theory directly, we use a program called RUN(Regularized Unfolding)[11] to unfold the detector effects.

Using the measured data as input, the unfolded Z p_T spectrum $\frac{1}{\sigma} \frac{d\sigma}{dp_T}$ is shown in FIG. 3. The measured Z p_T spectrum is also presented in the plot to show how much the unfolding changes the spectrum. The uncertainty shown in this plot is the statistical uncertainty only.

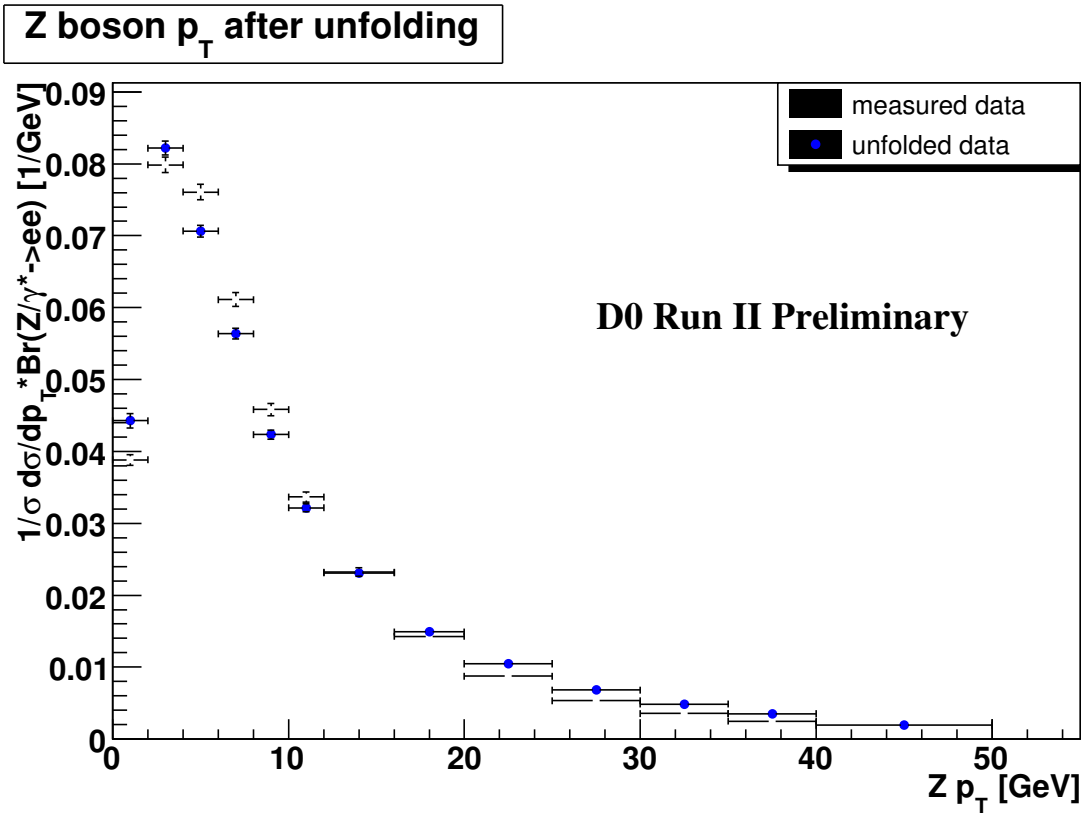


FIG. 3: Measured and unfolded spectra for the Z boson transverse momentum.

VIII. ESTIMATE OF SYSTEMATIC UNCERTAINTIES

The main uncertainties on the unfolded Z p_T spectrum arises from:

- understanding of the electron energy scale,
- understanding of the electron energy resolution,
- understanding of modelling of electron isolation and H-matrix efficiencies,
- parton distribution functions,
- and the unfolding method.

For the smearing parameters, energy scales, energy offsets and constant terms, the uncertainty on the unfolded Z p_T spectrum is estimated by varying each parameter by its standard deviation and noting the effect of the resulted Z p_T spectrum.

Uncertainties due to the parton distribution functions (PDF's) are estimated using the 40 distributions from CTEQ6.1m corresponding to twenty orthogonal parameters are shifted separately to their positive and negative 1σ limits.

There is an uncertainty associated with the unfolding program RUN. This is estimated using Monte Carlo. Instead of giving the program the data to unfold, we feed it the smeared Monte Carlo as the "data". The unfolded spectrum should be the same as the generator spectrum. The difference between them is used as the systematic uncertainty.

The largest current source of uncertainty, however, is the dependence of the efficiencies of the lepton identification requirements on the boson p_T , currently an 8% uncertainty. This uncertainty is under study.

The uncertainties from these sources are shown in Figure 4, along with the uncertainties from the Run I analysis. The largest current uncertainty is the dependence of the lepton isolation efficiencies on the boson p_T .

Fractional uncertainty for Run I and Run II

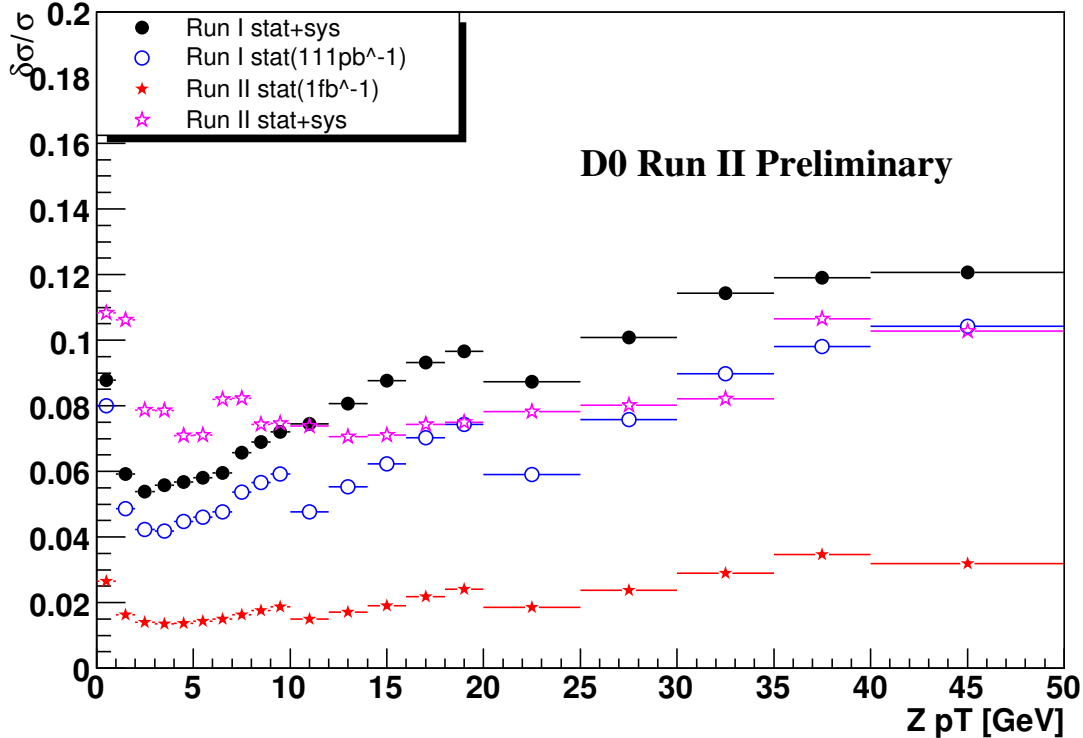


FIG. 4: Fractional systematic uncertainty on Z boson p_T distribution due to statistical uncertainty (red), combined statistical and systematic (pink) compared to values from the run i analysis statistical uncertainty (blue) and total (black). The Run II systematic uncertainties are being studied and are expected to be greatly reduced in the immediate future.

IX. RESULTS

The final $\frac{d\sigma}{dp_T}$ distribution, with both statistical and systematic uncertainties, is shown in Figure 5. The Z boson p_T spectrum for Z events that have rapidity >2 . is expected to be available soon.

-
- [1] J. Collins, D. Soper, G. Sterman, Nucl. Phys. B250 (1985) 199.
 - [2] C. Balazs, C.P. Yuan, Phys.Rev.D56:5558-5583,1997
 - [3] DØ Collaboration, B. Abbot *et al.*, Phys. Rev. D **61**, 032004 (2000).
 - [4] CDF Collaboration, T. Affolder *et al.*, Phys. Rev. Lett. **84**, 845 (2000).
 - [5] Stefan Berge, Pavel Nadolsky, Fredrick Olness, C.-P. Yuan, hep-ph/0410375
 - [6] V. Abazov *et al.*, submitted to Nucl. Instrum. Methods A, arXiv:0507191.
 - [7] η_{det} is the pseudorapidity of the electron candidate calculated using a vertex position of $z=0$ instead of the actual primary vertex position.
 - [8] R. Brun and F. Carminati, CERN Program Library Long Writeup W5013, 1993 (unpublished).
 - [9] C. Balazs and C.P. Yuan, Phys.Rev.D56:5558-5583,1997. [hep-ph/9704258]
 - [10] Elisabetta Barberio and Zbigniew Was, Comput. Phys. Commun 79,291 (1994)
 - [11] V. Blobel, The RUN manual, Regularized Unfolding for High-Energy Physics Experiments, program manual, unpublished

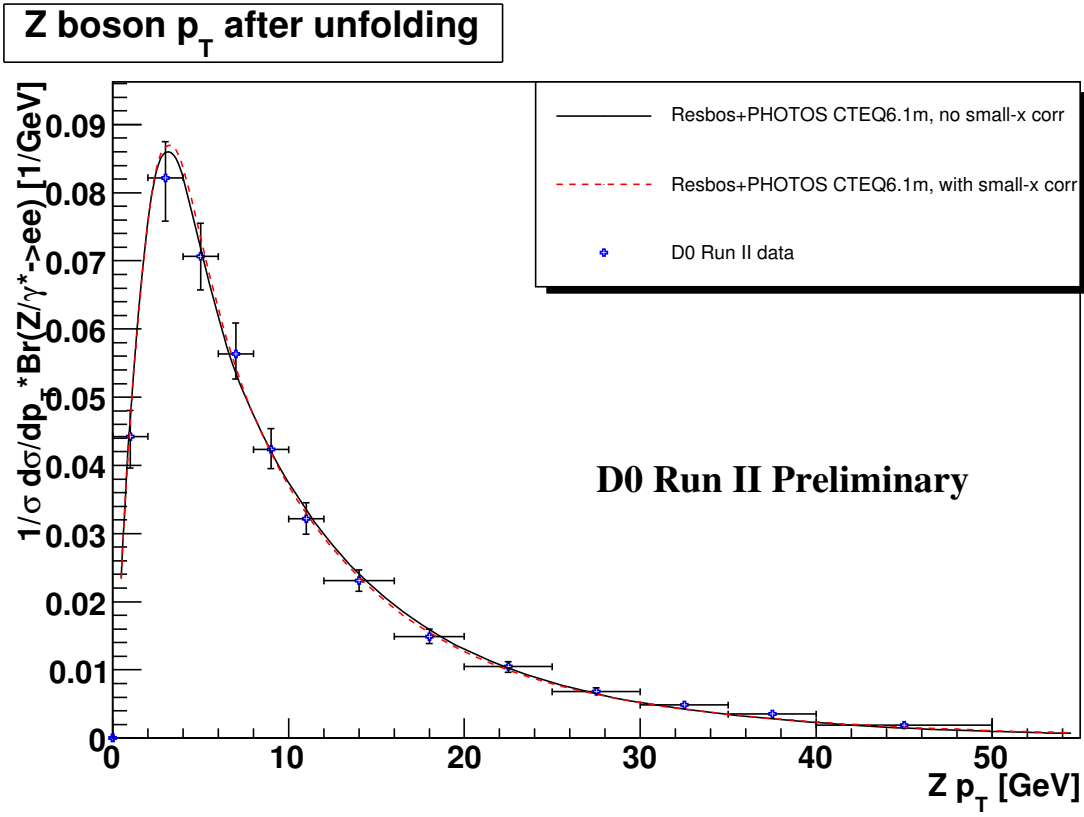


FIG. 5: Unfolded Z boson p_T distribution. The uncertainty contains both statistical and systematic uncertainties.